



Ion distribution dynamics near the Earth's bow shock: first measurements with the 2D ion energy spectrometer CORALL on the INTERBALL/Tail-probe satellite

Yu. I. Yermolaev, A. O. Fedorov, O. L. Vaisberg, V. M. Balebanov, Yu. A. Obod, R. Jimenez, J. Fleites, L. Llera, A. N. Omelchenko

► To cite this version:

Yu. I. Yermolaev, A. O. Fedorov, O. L. Vaisberg, V. M. Balebanov, Yu. A. Obod, et al.. Ion distribution dynamics near the Earth's bow shock: first measurements with the 2D ion energy spectrometer CORALL on the INTERBALL/Tail-probe satellite. *Annales Geophysicae*, 1997, 15 (5), pp.533-541. hal-00316237

HAL Id: hal-00316237

<https://hal.science/hal-00316237>

Submitted on 1 Jan 1997

HAL is a multi-disciplinary open access archive for the deposit and dissemination of scientific research documents, whether they are published or not. The documents may come from teaching and research institutions in France or abroad, or from public or private research centers.

L'archive ouverte pluridisciplinaire **HAL**, est destinée au dépôt et à la diffusion de documents scientifiques de niveau recherche, publiés ou non, émanant des établissements d'enseignement et de recherche français ou étrangers, des laboratoires publics ou privés.

Ion distribution dynamics near the Earth's bow shock: first measurements with the 2D ion energy spectrometer CORALL on the INTERBALL/Tail-probe satellite

Yu. I. Yermolaev¹, A. O. Fedorov¹, O. L. Vaisberg¹, V. M. Balebanov¹, Yu. A. Obod¹, R. Jimenez², J. Fleites², L. Llera², A. N. Omelchenko³

¹ Space Research Institute, Russian Academy of Sciences, Russia

² Intercosmos, Republic of Cuba

³ Institute of Applied Geophysics, Russian Hydrometeorological Service, Russia

Received: 20 May 1996 / Revised: 9 December 1996 / Accepted: 22 January 1997

Abstract. The dynamics of the ion distribution function near the Earth's bow shock is studied on the basis of quasi-3D measurements of ion energy spectra in the range of 30–24200 eV/q with the Russian-Cuban CORALL instrument on the INTERBALL/Tail-probe satellite. The instrument was designed for observations of magnetospheric plasma and measures ions, in an angular range of 36°–144° from the Earth-Sun direction. Ion populations generated by the Earth bow shock are often observed upstream from the bow shock. In the solar-wind stream compressed and heated by the passing of very dense magnetic cloud (CME), two types of these ion populations were measured upstream and before the bow shock crossing on 25 August 1995 at 07:37 UT. Both populations were observed in the energy range above 2 keV. At ~06:20 UT, when the angle between the direction of the interplanetary magnetic field and normal to the bow shock ϑ_{Bn} was $\simeq 43^\circ$ the instrument observed a narrow, fast (~800 km/s) field-aligned beam moving from the Earth. At ~07:30, when $\vartheta_{Bn} \simeq 28^\circ$, the wide ion pitch-angle distribution was observed. A similar suprathermal ion population is observed in the magnetosheath simultaneously with the solar-wind ion population being heated and deflected from the Sun-Earth direction. The similarity of observations during the mentioned time-interval and under usual solar-wind conditions allows us to conclude that types of suprathermal ion populations upstream and downstream from the bow shock do not depend on the solar-wind disturbance generated by magnetic cloud.

thermal and suprathermal ions in the Earth's magnetosphere and its environs are essential for understanding the structure and dynamics of the magnetosphere and its interaction with the solar wind (Yermolaev, 1994; Galeev *et al.*, 1995).

The solar wind is an important source of magnetospheric plasma and magnetospheric dynamics. Decelerated and heated on the bow shock, the solar-wind plasma interacts with the magnetopause and provides the mass, energy and momentum source for magnetospheric processes.

The magnetospheric dynamics are strongly coupled with the particle populations. Properties of magnetospheric plasma are controlled by the their sources, one of which is the solar wind, and by physical processes inside the magnetosphere: plasma may be heated and accelerated, beams are formed by acceleration of ionospheric plasma and by non-stationary processes in the tail plasma sheet and in the auroral region. The measurements of the velocity distribution of the hot ions is an important source of information on the dynamics of magnetospheric plasma, its sources and sinks, transport processes, and heating and acceleration. Of particular interest is the investigation of the thin boundaries that play a key role in the mass, momentum and energy-transfer processes between plasma domains.

The CORALL instrument was developed and built jointly by the Space Research Institute, Russia, and Intercosmos, Cuba. The scientific objectives of CORALL experiment are as follows:

1. To provide the 3D ion distribution function characteristics for the investigation of the dissipative and transport processes, and acceleration of ions at the plasma boundaries.
2. To provide measurements of magnetospheric ion populations, particularly of the plasma sheet in the geotail, for the investigation of dynamics and acceleration of the tail plasma.

In the present paper we embark on a study of the first group of problems, in particular, the physical processes

1 Introduction

The INTERBALL Project (a Tail probe with subsatellite launched on 3 August 1995 and an Auroral probe with subsatellite) focuses on the study of the energy, momentum and mass transport in critical regions of the solar wind/magnetosphere system. Measurements of

which are responsible for the appearance of ions with an energy a few times that of the solar wind near the Earth's bow shock.

Ions with energy higher than several keV upstream of the Earth's bow shock have been observed on many spacecraft and have been studied both theoretically and numerically; see reviews by Armstrong *et al.* (1985), Gosling and Robson (1985), Thomsen (1985), Krimigis (1987), Fuselier (1994). There are different types of these ion populations which are connected with the bow shock by interplanetary magnetic field lines and have different distribution functions.

Energetic (≥ 10 keV/q) ion beams are observed at the edge of the foreshock where the interplanetary magnetic field convected with the solar wind first encounters with the bow shock. Downstream from this boundary, low-energy (~ 1 keV/q) field-aligned ion beams are produced by reflection of a small fraction of the incident solar wind from the shock. The production of specularly reflected ion distribution is also observed here. The foreshock region upstream from the quasi-parallel bow shock is responsible for the production of energetic (or diffuse) ion distribution with an energy of a few keV/q extending to over 150 keV/q (Armstrong *et al.* 1985; Gosling and Robson 1985; Thomsen 1985; Krimigis 1987; Fuselier 1994). Energetic (≥ 3 keV/q) ions were also observed within the Earth's magnetosheath in the vicinity of the bow shock (Asbridge *et al.*, 1978).

The types and features of suprathermal ion distributions may depend on conditions in the solar wind and position of the bow shock. Unusual magnetic cloud or coronal mass ejection (CME) with very high proton density (up to 50 cm^{-3}) were observed on 24–25 August 1995. This magnetic cloud crossed the Earth's orbit on 25 August 1995 at ~ 02 UT and compressed and heated the solar wind and magnetosphere plasma. In the present paper different distributions of suprathermal ions observed upstream and downstream of the bow shock on 25 August 1995 at 07:37 UT are discussed in detail. Thus presented observations may lead to a better understanding of suprathermal ion populations under different conditions in the solar wind.

2 Instrument description

The plasma spectrometer CORALL measures ion characteristics in the energy-per-charge (E/q) range of 30–24200 eV/q. The fan-shaped field of view of the instrument $5^\circ \times 110^\circ$ is divided into five angular sectors. The combination of the large field of view and the spin of the satellite (spin axis is approximately directed towards the Sun, and the period of the spacecraft's rotation is about 120 s) allows one to measure the 3D ion distribution every 120 s. The accumulation time on one energy step is 1/1024th of the satellite rotation period, i.e. about 100 ms, and the scan period of one energy spectrum (32 steps) is equal to ~ 4 s.

The instrument consists of a nearly hemispherical electrostatic analyser (Gorn and Khazanov, 1979) followed by an MCP with five-sector collector (Fig. 1). The

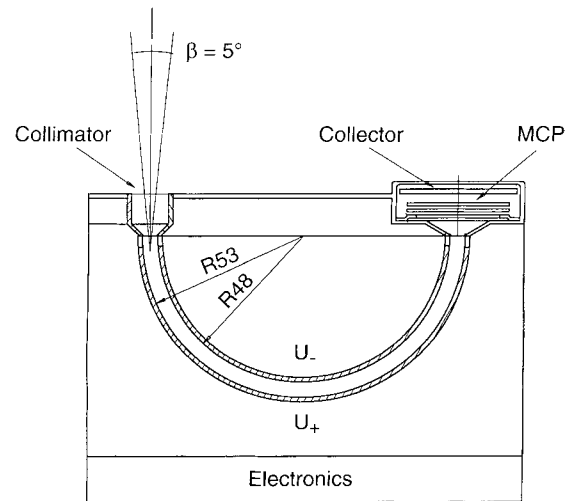


Fig. 1. Construction of hemispherical electrostatic analyser. Section plane is perpendicular to satellite spin axis

two concentric electrodes of the electrostatic analyser have radii of 4.8 and 5.3 cm. The parts of the 180° analyser are removed in order to set the entrance and exit aperture immediately at the edges of electrodes and to avoid ion trajectories which are not perpendicular to the edges (Fig. 2). The shape of electrostatic analyser and five-collector detector provide simultaneous measurements in five directions. The trajectories of two ions moving in one plane but at an angle of 110° relative to each other are shown schematically in Fig. 2. The potentials U varying in the range from 3 to 2420 V is applied to plates (a positive one, U_+ , for the outer electrode and a negative one, U_- , for the inner electrode). All interior surfaces of the electrostatic analyser are chromium-blackened in order to reduce the influence of scattered solar ultraviolet radiation. The output pulses of MCP's collectors are amplified by amplifiers with pulse discriminators, and are counted by individual counters.

The geometry of the electrostatic analyser was chosen for its mechanical simplicity, suitable energy passband and geometric factor, and its ability to provide angular distribution within a fan-shaped solid angle of view. The fan-shaped field of view is $5^\circ \times 110^\circ$ and is divided into sectors with central directions relative to the Earth-Sun line $42^\circ, 66^\circ, 90^\circ, 114^\circ$ and 138° .

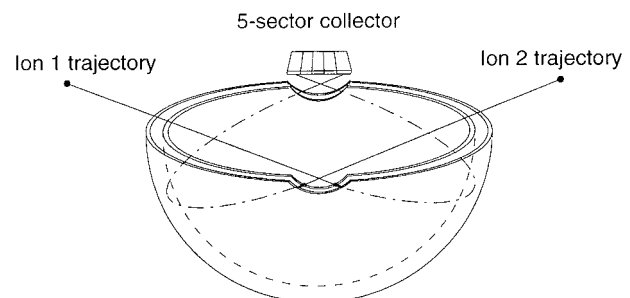


Fig. 2. Schematic view of analyser geometry and ion trajectories

The energy and angular resolutions were measured during calibration in laboratory facilities and are shown in Fig. 3. The full width at half maximum is 0.1 for energy bandwidth, and $5^\circ \times 25^\circ$ for azimuthal and polar angles, respectively. Neighbouring azimuthal channels overlap and calibration data are used to derive the angular distribution of ions. The 32 energy steps are evenly distributed over the energy range. The distance between successive energy steps is $(E_i - E_{i-1})/E_{i-1} = 24\%$. The geometric factors of the angular sector, determined by laboratory calibration, is $2.1 \cdot 10^{-3} \text{ cm}^2 \text{ sr}$. These values are cross-checked in flight with the use of the hot plasma environment. The sensitivity and dynamic range of the instrument is sufficient for comprehensive measurements of ions in the Earth's magnetosphere and its environs. Basic characteristics of instrument are presented in Table. 1.

The CORALL instrument was designed as an analyser of magnetospheric plasma. Similar instruments were on board ISEE-1 and ISEE-2 satellites at that time (Bame *et al.*, 1978), but these analysers could not obtain real 3D ion energy spectra and measured only near-equatorial plane distribution. The ion instruments of AMPTE UKS (Coates *et al.*, 1985) and AMPTE IRM (Paschman *et al.*, 1985) were improved and could obtain 3D spectra every spacecraft spin. But due to telemetry-rate limitations the processed data had a rough azimuthal and energy resolution. So the CORALL, measuring 3D ion spectra with azimuthal step 11° has an advantage in comparison with ISEE's instruments and can be used for magnetospheric and magnetosheath measurements as well as AMPTE's instruments.

Table 2 gives the numbers of energy steps (NE) and azimuthal sectors (NS) transmitted during one satellite rotation period. In sub-mode $G = 0$, the output data include all 32 (energy) \times 32 (azimuthal angle) counts of 5 channels for one rotation period (this sub-mode is similar to one in real-time telemetry mode). In other

Table 1. Technical characteristics of spectrometer CORALL

Energy range, eV/q	30–24200
Number of energy steps	32
$(E_i - E_{i-1})/E_{i-1}, \%$	24
Energy resolution, %	± 5
Number of polar channels	5
Polar angles, deg. from sun direction	42, 66, 90, 114, 138
Angular resolution:	
polar angle, deg.	± 25
azimuthal angle, deg.	± 5
Geometric factor, cm^2/sr	2.1×10^{-3}
Exposition time, s	0.1

cases the counts for neighbouring sectors and energy steps are summed in accordance with Table 2.

3 Results

The two top panels of Fig. 4 show the dynamics of ion energy spectra in 2 angular channels, CORALL 1 and 5 (42° and 138° relative to the Earth-Sun direction, respectively), on 25 August 1995: abscissa – UT time, ordinate axis – ion energy in keV. Colour indicates counts per 1.0 s and a colour table is presented at the right-hand side of the plot. The magnitude of the magnetic field is presented in the bottom panel of Fig. 4. Ion measurements were carried out in submode $G = 0$, i.e. with the highest energy and angular resolution. Data modulation (with period ~ 2 min) on dynamic spectrograms is due to satellite rotation.

From the beginning to 07:37 UT the satellite was in the solar wind: the main ion component exists only in a narrow cone near the Sun-Earth direction and is not registered by the CORALL instrument. Additionally, another (suprathermal) ion component with an energy of > 2 keV is observed during several time-intervals, moving in a direction different from that of the solar-wind flow. It should be noted that ion distributions in the time-interval 06:10–06:34 UT have a narrower energy range and higher flux than in subsequent time-intervals. At 07:37 UT the satellite crosses the Earth's bow shock and moves in the magnetosheath where the

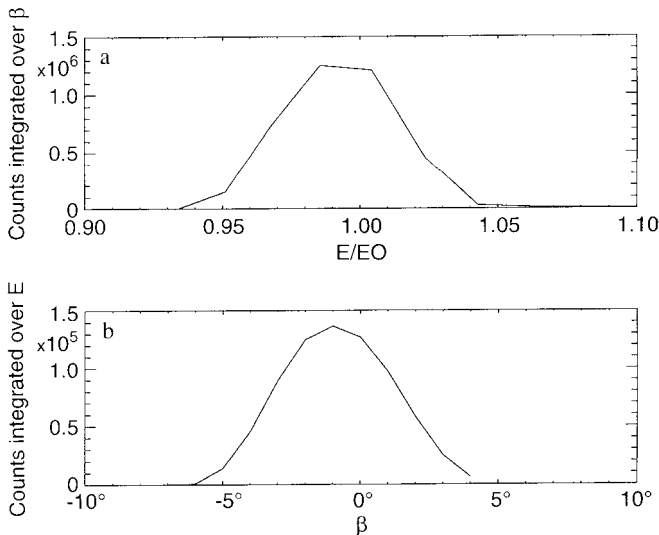


Fig. 3a, b. Results of laboratory calibration. **a** Curves for analyser energy response integrated over β angle and **b** β response integrated over energy

Table 2. The numbers of azimuthal sectors, NS, and of energy intervals, NE, in different modes of instrument and telemetry system

Instrument mode	instrument sub-mode	telemetry mode	NS	NE
non-processed	–	real time	32	32
	–	memory	32	32
processed	$G = 7$	real time	32	32
	$G = 0$	memory	32	32
	$G = 1$	memory	16	32
	$G = 2$	memory	16	16
	$G = 3$	memory	8	16
	$G = 4$	memory	4	16
	$G = 5$	memory	4	8
	$G = 6$	memory	4	4

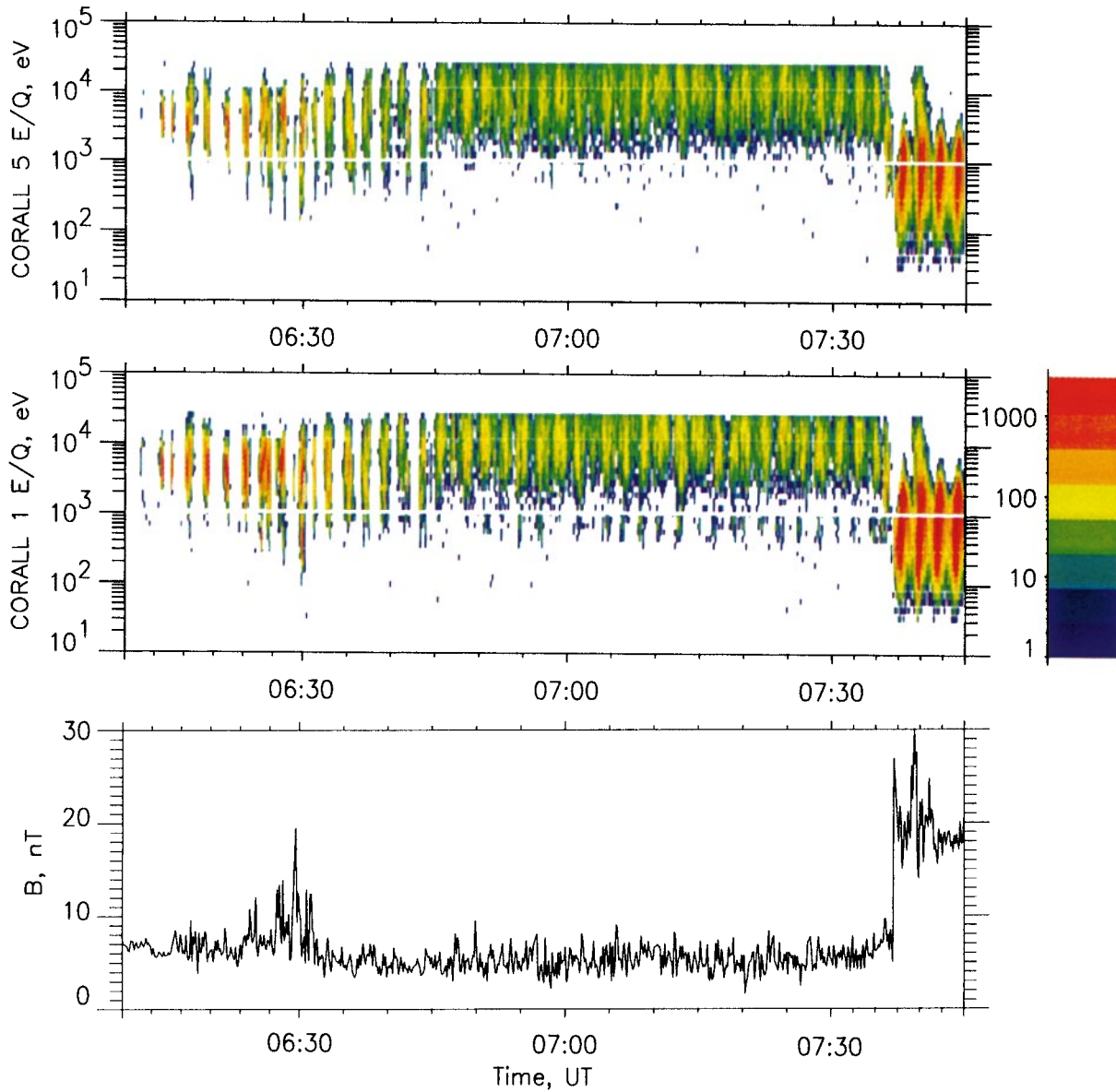


Fig. 4. Plasma and magnetic field for the time-interval 06:10–07:40 UT, 25 August 1995. *Top:* dynamics of ion spectra of 2 channels (CORALL 1 and CORALL 5 channels are oriented to directions which are nearest to solar and anti-solar directions, respectively). *Bottom:* magnitude of magnetic field

instrument observed solar-wind plasma which was heated, decelerated and deflected from Sun-Earth direction by the bow shock.

Figure 5 shows in more detail ion spectra and the magnitude of interplanetary magnetic field in the time-interval 06:10–06:40. Narrow (in energy and azimuthal angle) ion distribution with energy range of 1–20 keV/q is observed and is accompanied by large disturbances of the interplanetary magnetic field.

Pitch-angle distributions of ions and projection of this distribution on the $V_y - V_z$ plane (that is perpendicular to the Sun direction, with the y -axis lying in the same plane along the magnetic field projection) are shown in Fig. 6 for the time-interval marked by vertical lines in the previous figure. Both panels in Fig. 6 (and in the following figures) present distribution functions as

the density in the phase space. This figure shows that the ion beam has a narrow pitch-angle distribution and moves along magnetic field lines from the Earth with bulk velocity ~ 800 km/s (in supposition that observed ions are protons).

The dynamics of ion spectra and interplanetary magnetic field at the bow shock when the spacecraft moved from the solar wind into the magnetosheath are shown in Fig. 7 (the symbols are the same as in Fig. 5). The bow-shock crossing was at 07:37 UT when an abrupt change in the ion distribution function (the instrument began to measure large flux of low-energy shocked solar wind) and ramp of magnetic field are observed. Downstream from the bow shock the anisotropic flux of shocked solar-wind plasma is modulated by spacecraft rotation.

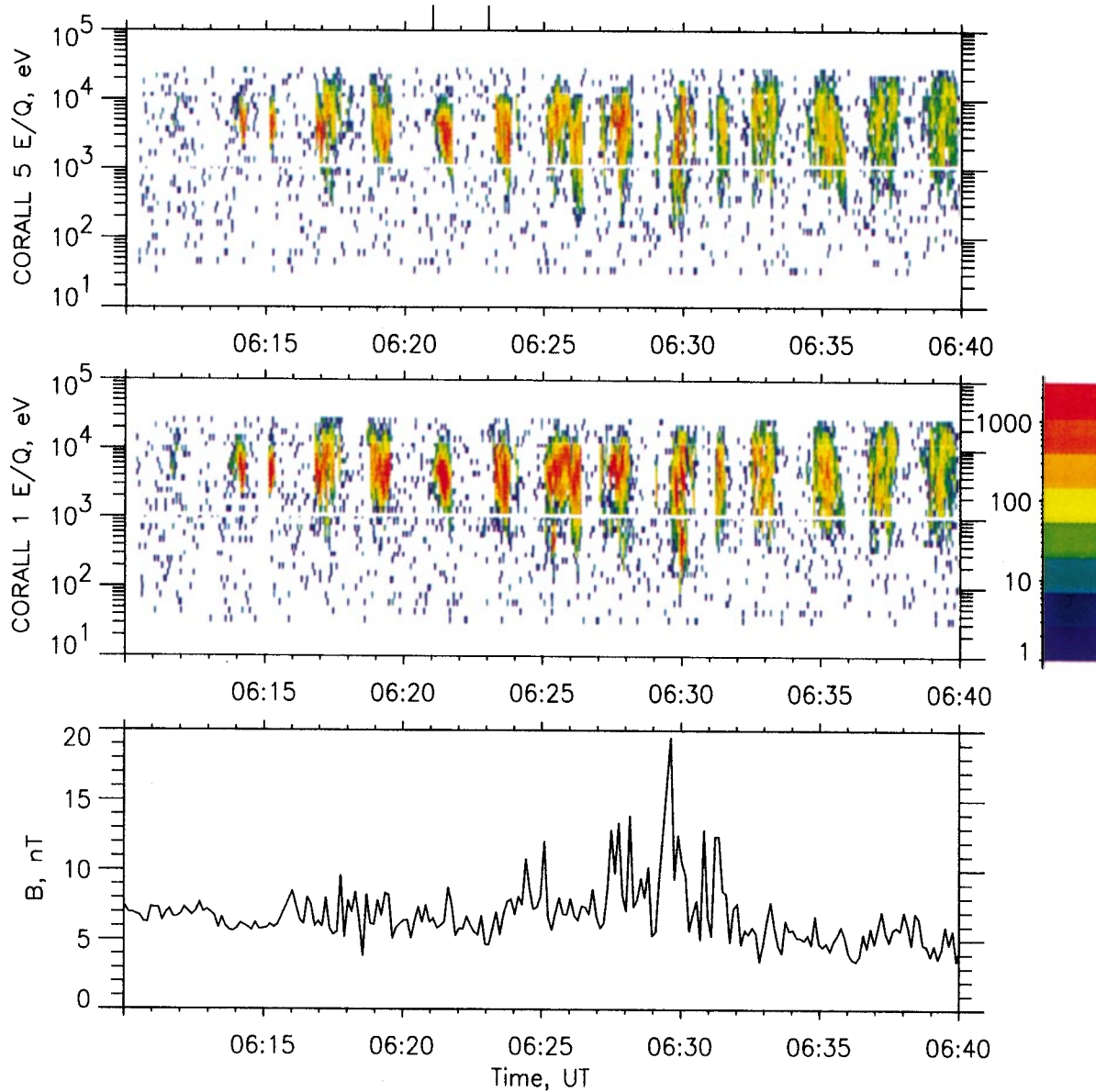


Fig. 5. Plasma and magnetic field for the time-interval 06:10–06:40 UT. *Top:* dynamics of ion spectra of 2 channels. *Bottom:* magnitude of interplanetary magnetic field

Pitch-angle distributions and $V_y - V_z$ distributions for the time-intervals marked by vertical lines are presented in Figs. 8 and 9, respectively. Figure 8 shows suprathermal ion distribution upstream from the bow shock. This ion population is observed at all pitch-angles and has a ring-like distribution in the $V_y - V_z$ plane. Nevertheless, the bulk velocity of this ion population is equal to ~ 400 km/s and is directed along the interplanetary magnetic field from the Earth.

Ion distribution downstream from the bow shock is presented in Fig. 9. The change in the ion distribution slope in the vicinity of $|V| \sim 800$ km/s shows that this distribution consists of two ion populations: a bell-like core, hot ($T_p \sim 250$ eV) and deflected from the Sun–Earth direction solar-wind plasma; and a flat tail, similar to the Fig. 8 suprathermal ion population which, in contrast with the previous figure, moves along magnetic

field line to the Earth. It is interesting to note that the suprathermal ion population was not observed so clearly during the first satellite rotation just after crossing the bow-shock front. It was registered during the second satellite rotation, disappeared for the next two rotations, reappeared, and so on.

4 Discussion and conclusions

The most important parameters influencing the type of ion suprathermal population upstream from the bow shock are the position of the spacecraft in the foreshock and orientation of the interplanetary magnetic field relative to the bow-shock normal (Gosling *et al.*, 1978; Gosling and Robson, 1985). The position of the satellite in the solar-ecliptic plane, components of average

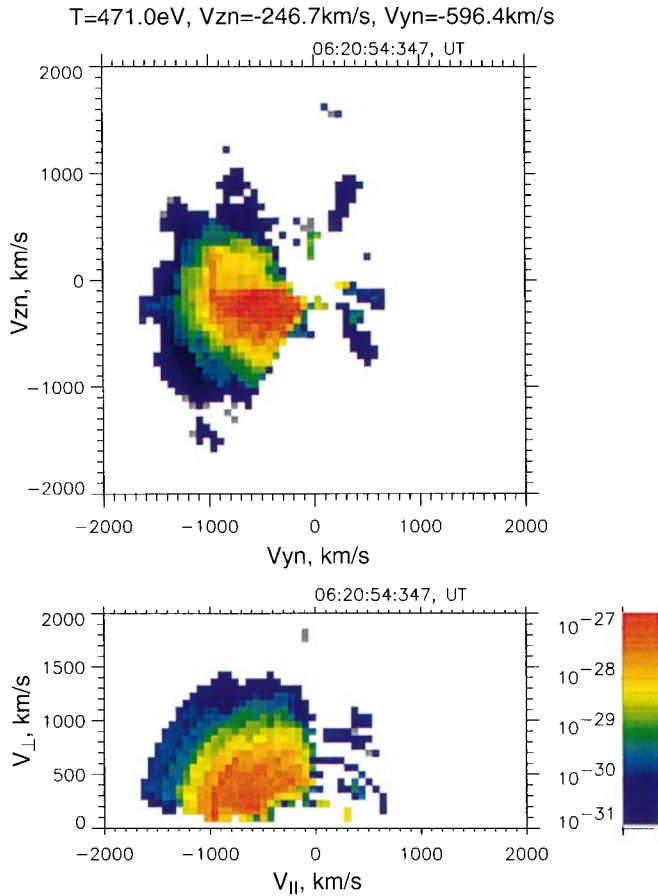


Fig. 6. Pitch-angle distribution (*top*) and $V_y - V_z$ (V_y is parallel to the IMF projection on the Y, Z_{SE} plane) distribution (*bottom*) for interval 06:19:22–06:21:41 UT

magnetic field and calculated angle between the interplanetary magnetic field and normal to the average bow shock ϑ_{Bn} for time-intervals shown in Figs. 6, 8 and 9 are presented in Table 3.

As is seen from the table, during three time-intervals the satellite was near the terminator in the ecliptic plane because $|Y_{SE}| \gg X_{SE}, Z_{SE}$. The average distance between the centre of the Earth and the bow shock in this region is about $26 R_E$ (Fairfield, 1971), but during our observations the distance was less than $20 R_E$. Observations on the INTERBALL/Tail probe with the VDP instrument show that on 25 August at 00 UT ion flux was very high, $14 \cdot 10^8 \text{ cm}^{-2} \text{ s}^{-1}$ (velocity 340 km/s, density 42 cm^{-3}), and at 04:30 UT flux remained high, $8 \cdot 10^8 \text{ cm}^{-2} \text{ s}^{-1}$ (Zastenker, personal communication,

1996). These data are confirmed by the WIND observations: in the time-interval of 01–08 UT when the satellite coordinates were approximately $4.2 \cdot 10^5 \text{ km}$ for X_{SE} , $-2.1 \cdot 10^5 \text{ km}$ for Y_{SE} and $-0.3 \cdot 10^5 \text{ km}$ for Z_{SE} , the ion flux decreased from 18 to $6.3 \cdot 10^8 \text{ cm}^{-2} \text{ s}^{-1}$. This unusually high pressure of solar wind is a possible cause of the unusual position of the bow shock during our observations. The WIND data show also that in the time-interval of 01–02 UT the proton temperature increased and magnitude of the magnetic field decreased in such a manner that the ratio of proton thermal to magnetic pressures β increased from ~ 0.5 up to 1.7 , and then β increased slowly up to ~ 2.5 at 08 UT. In accordance with the method of solar-wind-stream selection described by Yermolaev (1991, 1996), the WIND and INTERBALL observations indicate that on 25 August 1995 in the time-interval 01–02 UT both satellites crossed the boundary of magnetic cloud or coronal mass ejection (CME) and then measured compressed and heated plasma of solar wind. On one hand, moving disturbances in the solar wind are additional sources of energetic particles in the interplanetary space. On the other, the disturbed solar wind may result in a change in structure of the bow-shock front. In this case several features of bow shock and suprathermal ions observed near the bow shock may differ from features observed under quiet conditions in the solar wind.

Two factors, motion of the bow shock towards the Earth and the change of its shape (compression of its wings in the direction of the x -axis), lead to opposite changes of the normal's direction. We assume therefore that they may compensate each other, and orientation of the normal to the bow shock near the satellite position will remain close to that calculated from average shock shape. Under this assumption we calculated the angles ϑ_{Bn} presented in Table 3.

During the time-interval 06:00–06:35 UT, when $\vartheta_{Bn} \sim 43^\circ$, the spacecraft is located relatively close to the outer edge of ion foreshock (see Table 3). In this case the narrow field-aligned beam moving with bulk velocity $\sim 800 \text{ km/s}$ from the bow shock is observed. This observation is in good agreement with previous observations of suprathermal ions upstream from the Earth's bow shock (Armstrong *et al.*, 1985).

Another time-interval, 06:40–07:37 UT, is characterized by $\vartheta_{Bn} \sim 28^\circ$. As Table 3 shows, the satellite was in a region of quasi-parallel foreshock. In this region there is an ion population with higher energy (from 3 keV/q to higher than the upper limits of the instrument of 24 keV/q) and with all pitch-angles. This population has the

Table 3. Satellite position, magnetic field and angle ϑ_{Bn}

Time-intervals, UT	S/C coordinates, R_E			IMF components, nT			ϑ_{Bn} , deg.
	X_{SE}	Y_{SE}	Z_{SE}	B_X	B_Y	B_Z	
06:19:22–21:41	2.5	−19.3	0.9	0.5	6.8	2.2	43
07:27:38–29:57	2.5	−18.4	0.5	−5.4	1.7	2.3	28
07:39:22–41:41	2.5	−18.2	0.5	−11.5	−9.4	14.6	45

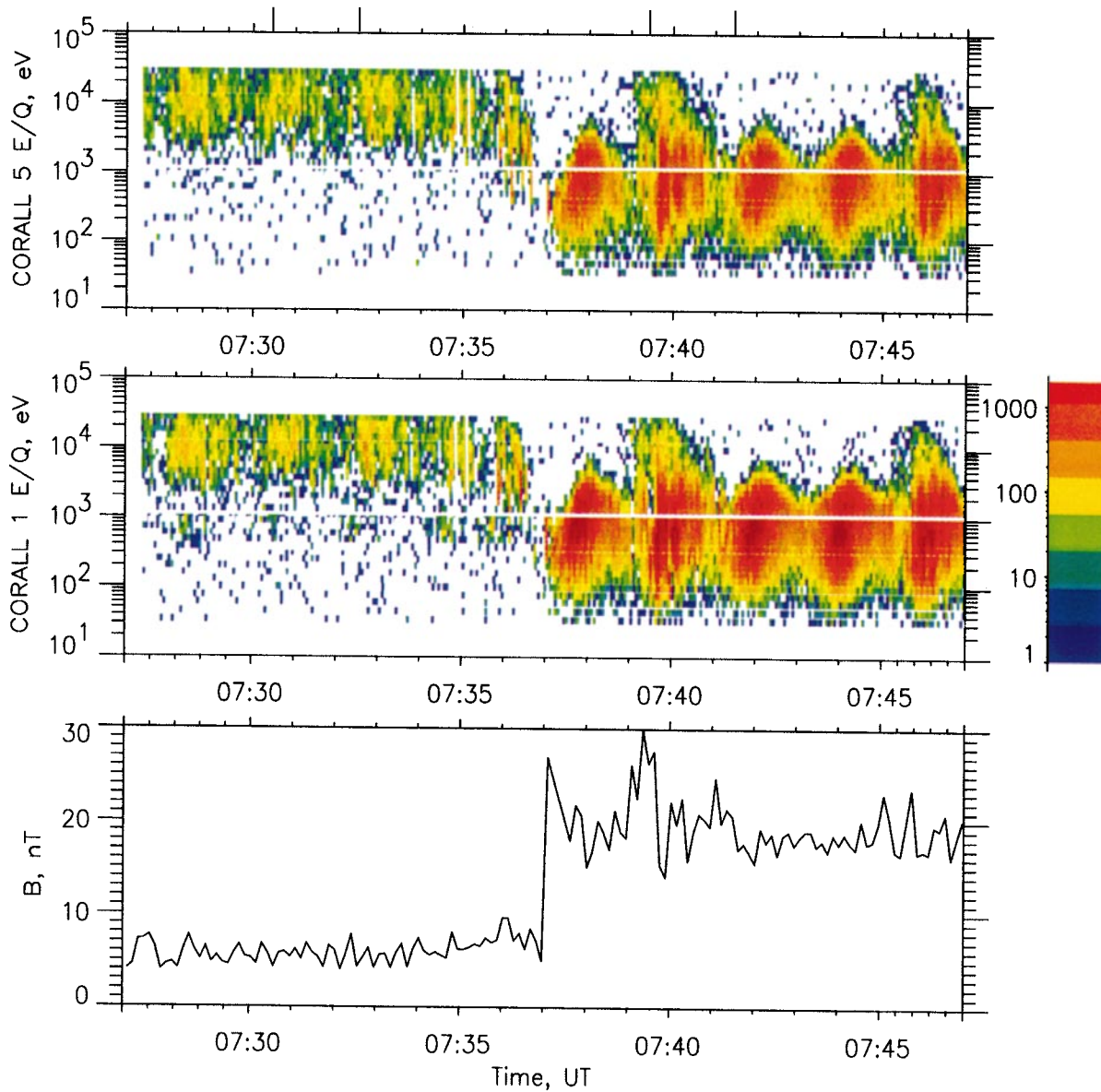


Fig. 7. Plasma and magnetic field for the time-interval 07:27–07:47 UT. *Top:* dynamics of ion spectra of 2 channels. *Bottom:* magnitude of interplanetary magnetic field

shape of a sphere and does not have high bulk velocity, ~ 400 km/s, which is directed along magnetic field line from the Earth's bow shock. This energetic ion population is likely to be classified as the diffuse distribution of suprathermal ions upstream from the bow shock (Gosling *et al.*, 1978).

Preliminary analysis shows that both types of suprathermal ion populations are likely to be similar to ones observed under quiet conditions in the solar wind. We hope that larger statistics of observation cases will allow us to compare some details of ion populations with different conditions in the solar wind.

Downstream from the bow shock (07:39–07:41 UT) in addition to hot solar-wind plasma the instrument measured suprathermal ion population, which is very similar to the diffuse ion population observed in the quasi-parallel foreshock under quiet conditions in the

solar wind. This ion population moved along the magnetic field line from the bow shock (i.e. towards the Earth). This fact supports the suggestion that this suprathermal ion population was generated by the bow shock. Although during the first satellite rotation period just after the bow-shock crossing this suprathermal ion population was not observed, we have many examples of measurements of this ion population downstream from the bow shock. Presented data agree with the suggestion of Asbridge *et al.* (1978) that the energetic ions are observed in the magnetosheath only under certain conditions upstream and downstream from the bow shock. So in future publications, with larger statistics, we will try to study the problem of whether this ion population is generated by the bow shock or by processes in the magnetosheath.

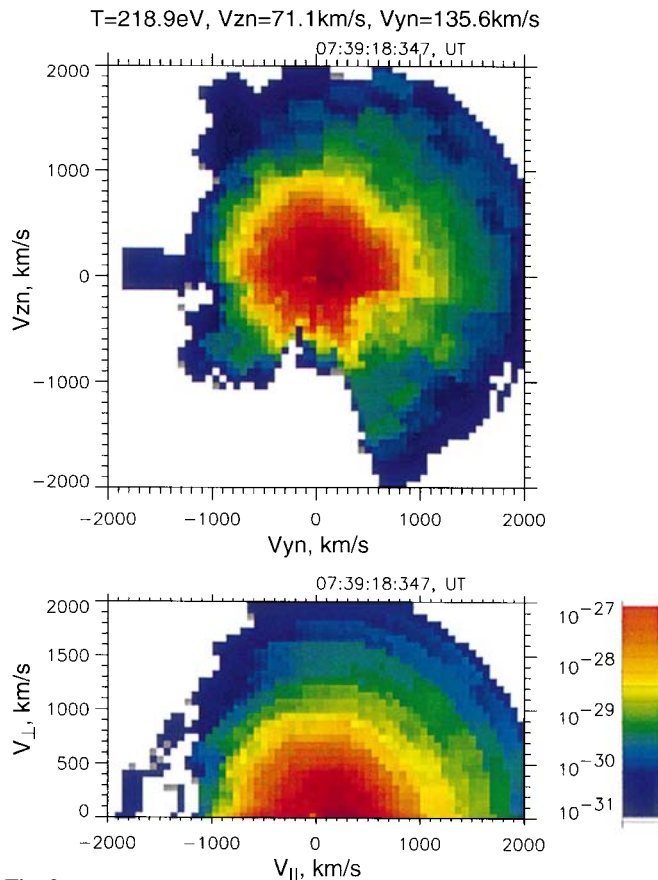
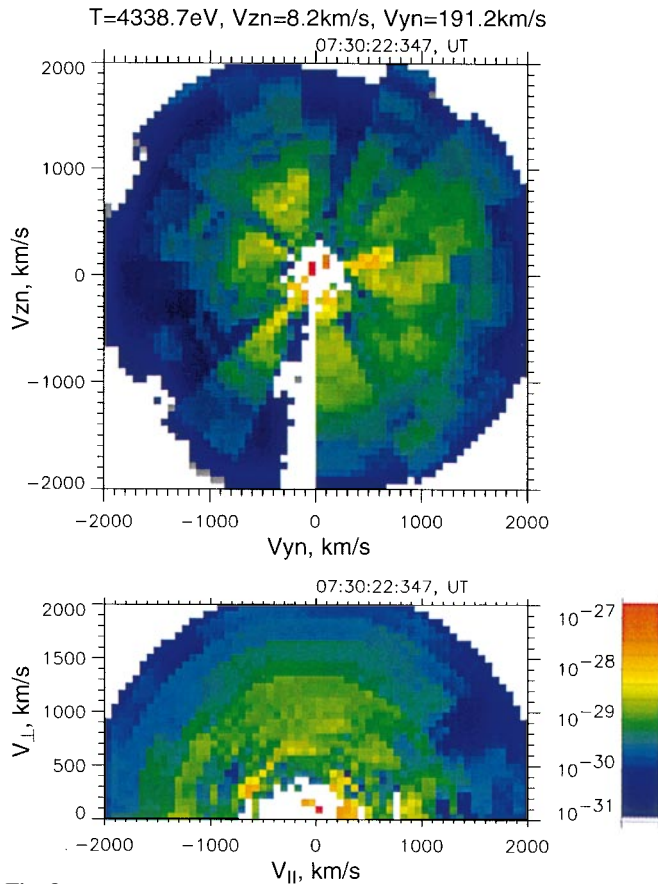


Fig. 8. The same as in Fig. 6 for time-interval 07:27:38–07:29:57 UT
Fig. 9. The same as in Fig. 6 for time-interval 07:39:22–07:41 UT

Acknowledgements. The authors would like to express their gratitude to V. E. Tsukerman, V. I. Uvarov, Yu. I. Laposov, V. D. Glaskov, A. Magrans, L. Sanchez, D. Madans, H. Borgess and to many other colleagues in Russia and Cuba for their help in the design, construction, testing and calibration of the CORALL experiment. The authors also thank G. N. Zastenker for VDP instrument data and L. M. Zelenyi and J. Büchner for useful comments on materials of present paper. Magnetic field data obtained with MIF magnetometer were provided by S. A. Romanov, N. E. Rybyeve and A. A. Skalsky. The WIND key parameter data of solar wind plasma and magnetic field (PIs are K. W. Ogilvie and R. P. Lipping) were provided by NASA Goddard Space Flight Center. This work was supported in part by INTAS-93-2931 Grant. The authors thank the second referee for very useful comments and suggestions on the manuscript.

Topical Editor K.-H. Glaßmeier thanks two referees for their help in evaluating this paper.

References

- Armstrong, T. P., M. E. Pesses, and R. B. Decker, Shock drift acceleration, in *collisionless shocks in the heliosphere: reviews of current research*, *Geophys. Monogr.*, **35**, 271, 1985.
- Asbridge, J. R., S. J. Bame, J. T. Gosling, G. Paschmann and N. Skopke, Energetic plasma ions within the Earth's magnetosheath, *Geophys. Res. Lett.*, **5**, 953, 1978.
- Bame, S. J., J. R. Asbridge, H. E. Felthausen *et al.*, ISEE-1 and ISEE-2 fast plasma experiment and the ISEE-1 solar wind experiment, *IEEE Trans. Geosci. Electron.*, **GE-16**, 3, 1978.
- Coates, A. J., J. A. Bowles, R. A. Goven, B. K. Hancock, A. D. Johnstone, and S. J. Kellock, The AMPTE UKS three-dimensional ion experiment, *IEEE Trans. Geosci. Rem. Sensing*, **GE-23**, 3, 1985.
- Fairfield, D. H., Average and unusual location of the Earth's magnetopause and bow shock, *J. Geophys. Res.*, **76**, 6700, 1971.
- Fuselier, S. A., Suprathermal ions upstream and downstream from the Earth's bow shock, in *Solar-wind sources of magnetospheric ultra-low-frequency pulsations*, *Geophys. Monogr.*, **81**, 107, 1994.
- Galeev, A. A., L. M. Zelenyi, and Yu. I. Galperin, The INTERBALL project to study solar-terrestrial physics, in *INTERBALL mission and payload*, RSA-IKI-CNES, p.11, 1995.
- Gorn, L. S., and B. I. Khazanov, *Spectrometry of ionizing emission aboard spacecraft*, Atomizdat, Moscow, 1979.
- Gosling, J. T., and A. E. Robson, Ion reflection, gyration, and dissipation at super-critical shocks, in *Collisionless shocks in the heliosphere: reviews of current research*, *Geophys. Monogr. Ser.*, **35**, 141, 1985.
- Gosling, J. T., J. R. Asbridge, S. J. Bame, G. Paschmann, and N. Skopke, Observations of two distinct populations of bow shock ions in the upstream solar wind, *Geophys. Res. Lett.*, **5**, 957, 1978.
- Krimigis, S. M., Observations of energetic ions and electrons at interplanetary shocks and upstream of planetary bow shocks by the Voyager spacecraft, *Proc. Int. Conf. Collisionless Shocks*, Ed K. Szego, Balatonfured, Hungary, p. 3, 1987.
- Paschman, G., H. Loidl, P. Obermayer, M. Ertl, *et al.* The Plasma instrument for AMPTE IRM, *IEEE Trans Geosci Rem. Sensing*, **GE-23**, 3, 1985.
- Thomsen, M. F., Upstream suprathermal ions, in *Collisionless shocks in the heliosphere: reviews of current research*, *Geophys. Monogr. Ser.*, **35**, 253, 1985.

- Yermolaev, Yu. I.**, Large-scale structure of solar wind and its relationship with solar corona: Prognoz 7 observations, *Planet. Space Sci.*, **39**, 1351, 1991.
- Yermolaev, Yu. I.**, Scientific program of solar and solar-wind observations: INTERBALL and Relict-2 missions, Proc. 3rd SOHO Worksh, Estes Park, USA, ESA SP-373, Ed. J. J. Hunt and V. Domingo, p. 441, 1994.

- Yermolaev, Yu. I.**, Transport of mass, momentum and energy from the Sun to the Earth by different types of solar wind streams, in *Solar drivers of interplanetary and terrestrial disturbances*, *Astronom. Soc. Pacific Conf. Ser.* **95**, Ed. K. S. Balasubramaniam, S. L. Keil, and R. N. Smartt, p. 288, 1996.